SPEKTRA: Jurnal Fisika dan Aplikasinya
Volume 9, Issue 2, August 2024
Homepage: doi.org/10.21009/SPEKTRA

DOI: doi.org/10.21009/SPEKTRA.092.05

Gravitational Lensing for A Spherically Symmetric Regular Charged Black Hole in Weak Field Limit

M. F. Shidik, H. S. Ramadhan*

Department Fisika, FMIPA, Universitas Indonesia, Depok, 16424, Indonesia

*Corresponding Author Email: hramad@sci.ui.ac.id

Received: 9 June 2024
Revised: 12 July 2024
Accepted: 28 August 2024
Online: 30 August 2024
Published: 30 August 2024

SPEKTRA: Jurnal Fisika dan Aplikasinya
p-ISSN: 2541-3384
e-ISSN: 2541-3392

ABSTRACT

Gravitational lensing is an integral part of the study of general relativity, as it is one of the direct consequences of general relativity. The existence of singularity within the black hole due to gravitational collapse is one of the key properties of the black hole. However, the introduction of non-linear electrodynamics (NLED) offers an intriguing possibility: nonsingular black holes. This work focuses on calculating the deflection angle within the weak field limit. Here, the photon's effective geometry associated with NLED is not incorporated; instead, the regular metric is utilized as it is, without presupposing its origins in NLED. A correction term in the deflection angle to the Reissner-Nordstrom (RN) case was found. This term manifests as a displacement in the position of the third image associated with the black hole.

Keywords: gravitational lensing, weak lensing, deflection angle, regular charged black hole

INTRODUCTION

The exploration of black holes remains intricately intertwined with the evolution of general relativity. The existence of the black hole itself was predicted through the General Relativity by solving Einstein's Equation. The presence of strong gravity around black holes produces interesting phenomena such as light deflection, a phenomenon where light bends due to following its geodesic in curved spacetime [1][2][3]. However, even with the presence of extreme gravitational conditions, light is only deflected a few arcseconds [4]. Nonetheless, the black hole is a good place to test General Relativity even further. Numerous observations have successfully pinpointed potential supermassive black holes in the cosmos. Recently, the Event Horizon Telescope (EHT) collaboration has been able to reconstruct the images of a potential supermassive black hole in the center of giant elliptical galaxy M87 [5] and our own Milky

Way Galaxy, Sagittarius A* [6]. These groundbreaking images are reconstructed using deflected light from background sources, illuminating the cosmic shadows cast by these supermassive entities

The deflection angle was first applied to the Schwarzschild black hole by Darwin [7]. Subsequently, efforts expanded to encompass various black hole models, such as the work by Fernando that studies the gravitational lensing for the Reissner-Nordstrom black hole [8]. However, unlike the precise calculations achieved by Darwin, the complexities inherent in different black hole models rendered direct solutions to the deflection angle equation unattainable without resorting to approximations. Recent studies have further extended this exploration to regular black holes with non-linear electrodynamics (NLED) sources, demonstrating that NLED can significantly modify the deflection angle compared to classical black hole models [9][10]. These findings suggest that gravitational lensing could serve as a distinguishing factor between different types of black holes, including those that are regular and those with singularities [11].

One of the defining properties of a black hole is the presence of singularity encapsulated within its horizon [12][13]. However, the introduction of non-linear electrodynamics (NLED) offers a tantalizing prospect: the construction of metrics that remain regular throughout, including all their invariants (for example, see [14]), unlike the previously mentioned Schwarzchild and Reissner-Nordstrom black hole which has a singularity at the origin [15]. Moreover, recent theoretical work has shown that NLED can lead to black holes with unique properties, such as "electromagnetic black holes," where photons can be trapped in a compact domain not exclusively governed by gravitational forces [16][17].

In this work, the weak deflection angle of a spherically symmetric regular charged black hole is calculated. By delving into these intricacies, this paper is aimed at shedding light on the profound implications of NLED on the fundamental nature of black holes and their observable characteristics. [9][10].

REGULAR CHARGED BLACK HOLE

To construct a regular charged black hole, the line element was considered for the static spherically symmetric metric

$$\mathrm{d}s^2 = -B(r)\mathrm{d}t^2 + A(r)\mathrm{d}r^2 + r^2(\mathrm{d}t^2 + \sin\theta\,\mathrm{d}\phi^2) \tag{1}$$

where

$$B(r) = A(r)^{-1} = 1 - \frac{2m(r)}{r}. \tag{2}$$

Here, $m(r)$ is the mass function expressed as

$$m(r) = \frac{\sigma(r)}{\sigma_\infty}M, \tag{3}$$

where $\sigma_\infty \equiv \sigma(r \to \infty)$. The distribution function $\sigma(r)$ should satisfy $\sigma(r) > 0$ and $\sigma'(r) > 0$ for $r \geq 0$. The normalization factor is taken such that

$$\frac{\sigma(r)}{r} \to 0 \tag{4}$$

at $r \to 0$. Additionally, the metric function can be extended by employing an additional factor $\gamma > 0$ to the variable r. The mass function then takes the form of

$$m(r) = \left(\frac{\sigma(\gamma r)}{\sigma_\infty}\right)^\gamma M. \tag{5}$$

Following the works from Balart [14], the following distribution function

$$\sigma(r) = \left(\exp\left(\frac{Q^2}{Mr}\right) + 1\right)^{-1} \tag{6}$$

is choosen and $\gamma = 5$ is taken. Here, $\sigma_\infty \to 2$. It can easily be verified that, asymptotically, the metric approaches RN, with

$$f(r) = 1 - \frac{2m(r)}{r} \approx 1 - \frac{2M}{r} + \frac{Q^2}{r^2}. \tag{7}$$

The event horizons can be determined by solving the roots of

$$f(r) = 0, \tag{8}$$

which can be calculated numerically. The maximum charge for this metric function happens when $|Q| = 1.162M$.

The source of the Einstein field equation from this metric function corresponds to an NLED model. The NLED model is a function of Maxwell's Lagrangian $L = L(F)$, where $F \equiv \frac{1}{4}F_{\mu\nu}F^{\mu\nu}$. In the weak field limit, this model should be compatible with Maxwell equation, $L = -F$ [18].

DEFLECTION ANGLE FOR SPHERICALLY SYMMETRIC BLACK HOLE

The trajectory of light can be obtained from solving the null geodesic EQUATION (9). Using the general spherically symmetric metric, it was found that the light equation of motion could be expressed as follows:

$$\frac{A(r)}{r^4}\left(\frac{\mathrm{d}r}{\mathrm{d}\phi}\right)^2 + \frac{1}{r^2} - \frac{1}{b^2 B(r)} = 0. \tag{9}$$

The deflection of light due to the presence of massive object can be seen in FIGURE 1 [19].

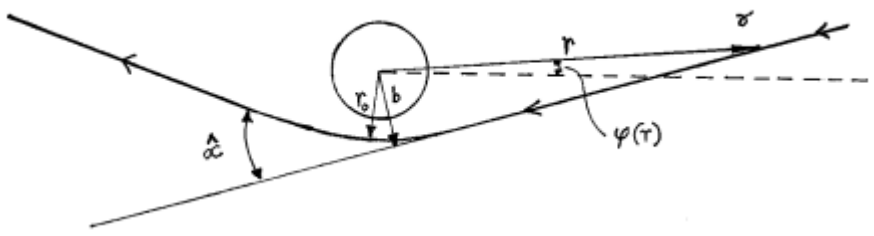

FIGURE 1. The bending of light under the influence of gravitational field of massive source.

Here b represents the impact parameter, while r_0 signifies the closest approach (extremum) of the light trajectory, implying $dr/d\phi = 0$ at r_0. Using this condition, the relationship between the impact parameter and the closest approach is derived as follows:

$$b = r_0\big(B(r_0)\big)^{-1/2}. \tag{10}$$

The total deflection angle then can be expressed as

$$\begin{aligned}\hat{\alpha} &= 2|\phi(r) - \phi(\infty)| - \pi \\ &= 2\int_{r_0}^{\infty} A^{1/2}(r)\left[\left(\frac{r}{r_0}\right)^2\left(\frac{B(r)}{B(r_0)} - 1\right)\right]^{-1/2}\frac{\mathrm{d}r}{r} - \pi.\end{aligned} \tag{11}$$

The black hole shadow can be approximated using the lens equation. The geometry is shown in FIGURE 2 [8].

Here β is the angular position of the source from the observer, on the other hand θ is the angular position of the images due to the gravitational lens. Under the weak-field limit, the thin lens approximation can be employed to calculate the position of the images. From FIGURE 2, the full lens equation can be written as

$$D_s \tan\theta = D_s \tan\beta + D_{ds}[\tan\theta + \tan(\hat{\alpha} - \theta)]. \tag{12}$$

EQUATION (12) is the Virbhadra-Ellis lens equation [4]. Since the deflection angle is small, the small angle approximation can be applied, and the lens equation can be written as follows:

$$\beta = \theta - \hat{\alpha}\frac{D_{ds}}{D_d}. \tag{13}$$

The magnification μ is defined as the ratio of the image area to the source area

$$\mu = \frac{\mathrm{d}\theta}{\mathrm{d}\beta}\frac{\theta}{\mu}. \tag{14}$$

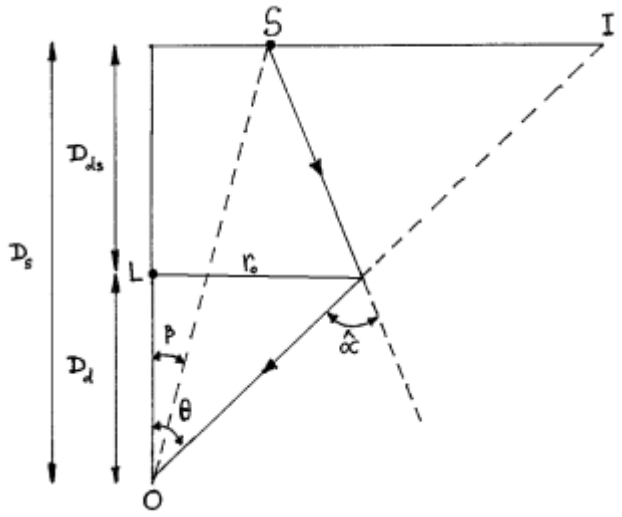

FIGURE 2. The geometry of lensing. Here S, O, and L are the source image, the observer, and the lens (black hole) respectively.

RESULTS AND DISCUSSION

Integrating EQUATION (11) exactly yields divergent term. To circumvent it, the term inside the square bracket is expanded up to the fourth order. Note that this expansion is valid only in the weak field limit when $b \gg r_+$. Here, this expression is obtained.

$$\left(\frac{r}{r_0}\right)^2\left(\frac{B(r)}{B(r_0)}-1\right) \approx 1-\frac{2Mr}{r_0^2+r_0r}+\frac{Q^2}{r_0^2}-\frac{4M^2}{r_0^2+r_0r}-\frac{8M^3}{r_0^2r+r_0r^2}+\frac{2MQ^2(2r_0+r)}{r_0^2r(r_0+r)} -\frac{Q^4(r_0^2+r_0r+r^2)}{5r_0^3Mr(r_0+r)}-\frac{16M^4}{r_0r^2(r_0+r)}-\frac{Q^4(9r_0^2+7r_0r+2r^2)}{5r_0^3r^2(r_0+r)} +\frac{4M^2Q^2(3r_0+r)}{r_0^2r^2(r_0+r)}+\frac{Q^6(r_0^2+r^2)}{60M^2r_0^4r^2}. \quad (15)$$

After a long but straightforward integral, the total deflection angle can be expressed as

$$\hat{\alpha} = \frac{4M}{r_0}+\frac{M^2}{r_0^2}\left(-4+\frac{15}{4}\pi\right)-\frac{3\pi Q^2}{4r_0^2}+\frac{M^3}{r_0^3}\left(\frac{122}{3}-\frac{15}{2}\pi\right)+\frac{MQ^2}{r_0^3}\left(-14+\frac{3}{2}\pi\right) +\frac{M^4}{r_0^4}\left(-130+\frac{3465}{64}\pi\right)+\frac{Q^4}{r_0^4}\left(-2+\frac{141}{64}\pi\right)+\frac{M^2Q^2}{r_0^4}\left(50-\frac{825}{32}\pi\right) +\frac{\pi Q^6}{64r_0^4M^2}. \quad (16)$$

FIGURE 3 shows the comparison of total deflection angle. The NLED increase the total deflection angle, but as r_0 is increased, the total deflection angle begins to approach the Reissner-Nordstrom deflection angle. Changing the mass to charge ratio does affect the total deflection angle as shown by FIGURE 4. But the general behaviour of the total deflection angle remains the same.

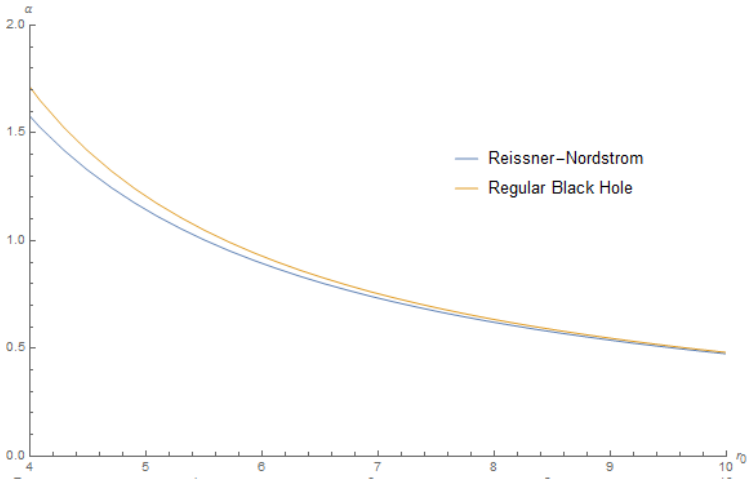

FIGURE 3. Total deflection angle of Reissner-Nordstrom and regular charged black hole, both with $Q^2/M^2 = 1/2$.

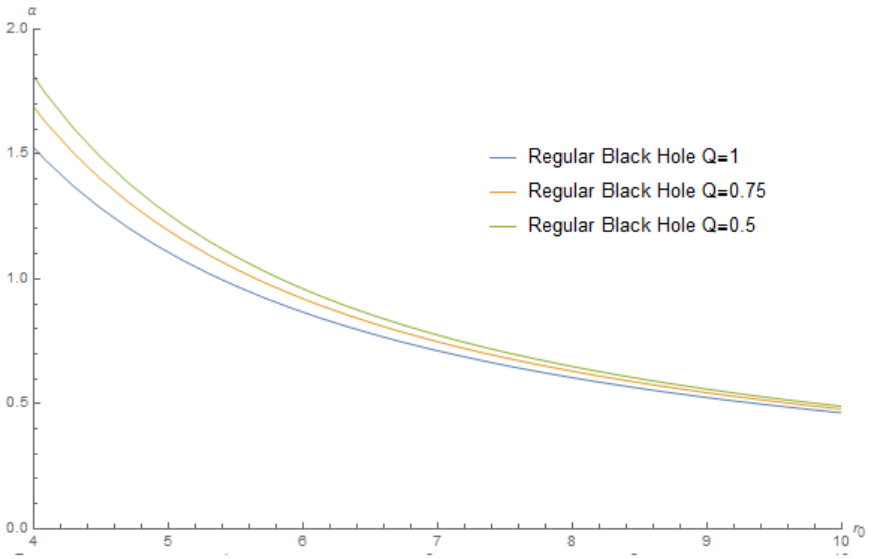

FIGURE 4. Total deflection angle of regular charged black hole with various charge

It can be seen from FIGURE 4 that the deflection angle decreases as the black hole charge increases. But it must be noted that this deflection angle takes into account the contribution of the whole metric function. A similar pattern can also be observed in the Reissner-Nordstrom black hole. FIGURE 5 however show the difference in NLED contribution with Reissner Nordstrom black hole.

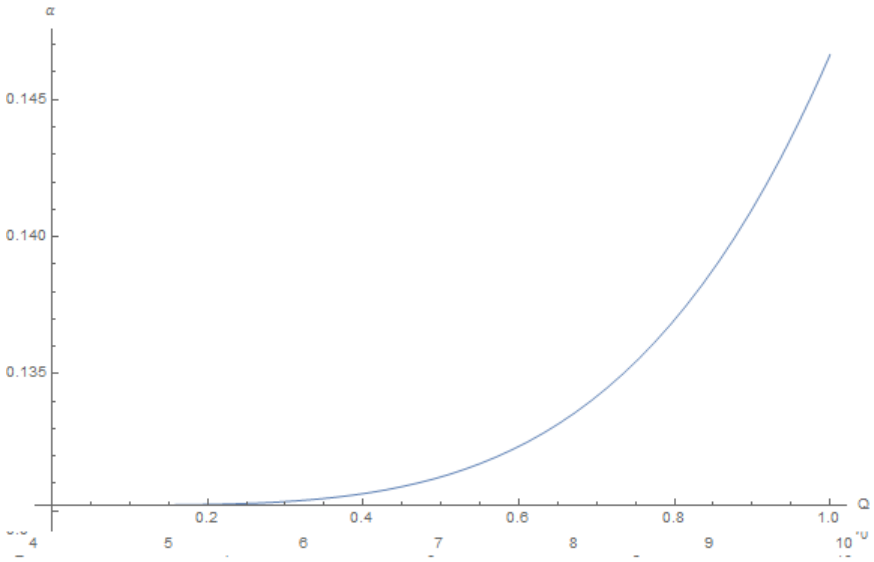

FIGURE 5. Extra term contribution to total deflection angle when $\boldsymbol{r_0 = 4}$.

Only $r_0 = 4$ is considered since the photon sphere of this metric function located at $r = 3 \rightarrow 1.74306$, depending on the value of black hole charge. Consideration must also be given to the fact that the approximation close to the photon sphere may yield higher error due to the weak field approximation. It is observed that the contribution from the extra term increases rapidly as the charge is increased. However, the contribution is not sufficient to offset the

contribution from the whole metric function; hence, it is still observed that the total deflection angle decreases as the charge is increased.

Having computed the total deflection angle, our next step is to determine the position of the images of the black hole. This entails specifying certain parameters of the black hole. In this study, the parameter of the supermassive black hole identified by Fritteli [20] is followed, where the black hole's mass is denoted as $M = 2.8 \times M_{\odot}$. Here, the ratio $D_{ds} \; / \; D_d \; = 1 \; / \; 2$ is taken, while the distance from the black hole to the observer $D_d = 8.5$ kpc. Furthermore, the condition that the charge $Q^2 = M^2 \; / \; 2$ is assumed. Utilizing these specified assumptions, the image position of the regular charged black hole is then computed.

TABLE 1. Image position due to gravitational lensing.

Source Position	Reissner-Nordstrom			Regular Charged Black Hole		
	First Image	Second Image	Third Image	First Image	Second Image	Third Image
10^{-4}	-1.15577	1.15587	-4.91901×10^{-6}	-1.15577	1.15587	-5.96732×10^{-6}
10^{-3}	-1.15532	1.15632	-4.91901×10^{-6}	-1.15532	1.15632	-5.96732×10^{-6}
10^{-2}	-1.15083	1.16083	-4.91901×10^{-6}	-1.15083	1.16083	-5.96732×10^{-6}
10^{-1}	-1.10690	1.20690	-4.91901×10^{-6}	-1.10690	1.20690	-5.96732×10^{-6}
1	-0.759329	1.75933	-4.91902×10^{-6}	-0.759329	1.75933	-5.96733×10^{-6}
2	-0.528367	2.52837	-4.91903×10^{-6}	-0.528367	2.52837	-5.96734×10^{-6}
3	-0.39367	3.39365	-4.91905×10^{-6}	-0.39367	3.39365	-5.96735×10^{-6}
4	-0.309956	4.30996	-4.91906×10^{-6}	-0.309956	4.30996	-5.96737×10^{-6}
5	-0.254249	5.25425	-4.91907×10^{-6}	-0.254249	5.25425	-5.96738×10^{-6}

TABLE 1 shows the regular black hole only shifts the image position, particularly affecting the third one. The patterns of the first and second images remain unaltered in comparison to the RN model. With increasing source positions, the first image gradually shifts closer to the optical axis, while the second image moves farther away from it. Remarkably, regardless of changes in the source position, the second image maintains a consistent location.

TABLE 2. Magnification of images due to gravitational lensing.

Source Position	Reissner-Nordstrom			Regular Charged Black Hole		
	First Image	Second Image	Third Image	First Image	Second Image	Third Image
10^{-4}	-5778.6	5779.6	5.33164×10^{-13}	-5778.6	5779.6	7.44784×10^{-13}
10^{-3}	-577.41	578.41	5.33164×10^{-14}	-577.41	578.41	7.44784×10^{-14}
10^{-2}	-57.2926	58.2926	5.33164×10^{-15}	-57.2926	58.2926	7.44784×10^{-15}
10^{-1}	-5.29531	6.29531	5.33165×10^{-16}	-5.29531	6.29531	7.44785×10^{-16}
1	-0.228925	1.22892	5.33172×10^{-17}	-0.228925	1.22892	7.44795×10^{-17}
2	-0.0456654	1.04567	2.6659×10^{-17}	-0.0456654	1.04567	3.72403×10^{-17}
3	-0.0136386	1.01364	1.77629×10^{-17}	-0.0136386	1.01364	2.48272×10^{-17}
4	-0.00519891	1.0052	1.33299×10^{-17}	-0.00519891	1.0052	1.86207×10^{-17}
5	-0.00234707	1.002019	1.06641×10^{-17}	-0.00234707	1.002019	1.48968×10^{-17}

From TABLE 2, it is observed that the magnification drops significantly as the source position increases. Hence, it would be harder to observe the image as the source position increases. The

magnification of the third image also has very low magnification compared to the other images. This condition leads to the third image become harder to observe and observer may mistakenly to see only two images.

Similar to image position, there is no change in the behavior of the magnification compared to Reisner Nordstrom black hole, as the magnification rapidly decreases with an increase in the source position. However, it can be seen that NLED results in a very small increase in the magnifaction. The increase is very small that it might be hard to notice during observation.

CONCLUSION

From this research, it was found that NLED modifies the light geodesic, thereby introducing an additional term in the form of $14M^3 / 3r_0^3 + 44M^4 / 3r_0^4 - 2Q^4 / r_0^4 + 8Q^4 / 15r_0^3M + 21\pi Q^4 / 16r_0^4 - \pi Q^6 / 64r_0^4M^2$ to the total deflection angle. The change in the total deflection angle can be observed by the translational shift in the third image position compared to Reissner-Nordstrom black hole, while the first and second image as well as the behavior of the image position remain unchanged. An increase, albeit very small and potentially negligible, in the image magnification was also observed.

ACKNOWLEDGMENTS

We thank Afrasiab Durrani and Hassan Uddin for fruitful discussions. This research is supported by the Hibah Riset FMIPA UI No. PKS-026/UN2.F3.D/PPM.00.02/2023.

REFERENCES

[1] S. Zschocke, "Light deflection in binary stars," *The Astronomical Journal*, vol. 144, no. 3, p. 77, Sep. 2012, doi: 10.1088/0004-6256/144/3/77.

[2] S. Zschocke, "Total light deflection in the gravitational field of an axisymmetric body at rest with full mass and spin multipole structure," *Physical Review D*, vol. 107, no. 12, p. 124055, Jun. 2023, doi: 10.1103/PhysRevD.107.124055.

[3] E. B. Manoukian and E. B. Manoukian, "Light Deflection in GR and Gravitational Lensing: Prerequisite Chap. 56," in *100 Years of Fundamental Theoretical Physics in the Palm of Your Hand: Integrated Technical Treatment*, Cham: Springer, pp. 367-371, 2020, doi: 10.1007/978-3-030-51081-7_57.

[4] K. S. Virbhadra and George F. R. Ellis, “Schwarzschild black hole lensing,”, *Physical Review D*, vol. 62, no. 8, p. 084003, Sep. 2000, doi: 10.1103/PhysRevD.62.084003.

[5] K. Akiyama et al., “First m87 event horizon telescope results. I. the shadow of the supermassive black hole”, *The Astrophysical Journal Letters*, vol. 875:L1, no. 1, 17pp, Apr. 2019, doi: 10.3847/2041-8213/ab0ec7.

[6] K. Akiyama et al., “First sagittarius a* event horizon telescope results. i. the shadow of the supermassive black hole in the center of the milky way,” *The Astrophysical Journal Letters*, vol. 930:L12, no. 2, 21pp, May 2022, doi: 10.3847/2041-8213/ac6674.

[7] C. G. Darwin, “The gravity field of a particle,” in *Proceedings of the Royal Society London* in Series A. Mathematical, Physical & Engineering Sciences, vol. 249, no. 1257, pp. 180–194, Jan. 1959, doi: 10.1098/rspa.1959.0015.

[8] S. Fernando and S. Roberts, “Gravitational lensing by charged black holes,” *General Relativity and Gravitation*, vol. 34, no. 8, pp. 1221-1230, Aug. 2002, doi: 10.1023/A:1019726501344.

[9] T. Manna, et. al., "Strong lensing of a regular black hole with an electrodynamics source," *General Relativity and Gravitation*, vol. 50, no. 54, pp. 1-18, Apr. 2018, doi: 10.1007/s10714-018-2375-3.

[10] J. Liang, "Strong gravitational lensing by regular electrically charged black holes," *General Relativity and Gravitation*, vol. 49, no. 137, pp. 1-18, Oct. 2017, doi: 10.1007/s10714-017-2307-7.
[11] M. S. Churilova and Z. Stuchlik, "Quasinormal modes of black holes in 5D Gauss–Bonnet gravity combined with non-linear electrodynamics," *Annals of Physics*, vol 418, pp. 1-13, July 2020, doi: 10.1016/j.aop.2020.168181.
[12] Y. Kumaran and A. Övgün, "Shadow and deflection angle of asymptotic magnetically-charged non-singular black hole," *The European Physical Journal C*, vol. 83, no. 9, pp. 1-23, Sep. 2023, doi: 10.1140/epjc/s10052-023-12001-z.
[13] R. Carballo-Rubio, F. Di Filippo, S. Liberati, and M. Visser, "Singularity-free gravitational collapse: From regular black holes to horizonless objects," in *Regular Black Holes: Towards a New Paradigm of Gravitational Collapse*, Singapore: Springer Nature Singapore, pp. 353-387, 2023, doi: 10.1007/978-981-99-1596-5_9.
[14] L. Balart and E. C. Vagenas, "Regular black holes with a nonlinear electrodynamics source," *Physical Review D*, vol. 90, no. 12, p. 124045, Dec. 2014, doi: 10.1103/PhysRevD.90.124045.
[15] C. Lan, H. Yang, Y. Guo, and Y-G. Miao, "Regular black holes: A short topic review," *International Journal of Theoretical Physics*, vol. 62, no. 9, p. 202, Sept. 2023, doi: 10.1007/s10773-023-05454-1.
[16] H. El moumni, K. Masmar, and A. Övgün, "Weak deflection angle of some classes of non-linear electrodynamics black holes via Gauss-Bonnet theorem," *Int. J. Geom. Meth. Mod. Phys.*, vol. 19, no. 06, p. 2250094, 2022, doi: 10.1142/S0219887822500943.
[17] C. Lämmerzahl, M. Maceda, and A. Mac'ias, "On slowly rotating black holes and nonlinear electrodynamics," *Classical and Quantum Gravity*, vol. 36, no. 1, p. 015001, Nov. 2018, doi: 10.1088/1361-6382/aaeca7.
[18] A. S. Habibina and H. S. Ramadhan, "Geodesic of nonlinear electrodynamics and stable photon orbits," *Phys. Rev. D*, vol. 101, no. 12, p. 124036, June 2020, doi: 10.1103/PhysRevD.101.124036.
[19] S. Weinberg, "*Gravitation and cosmology: Principles and applications of the general theory of relativity*," J. Wiley, 1972.
[20] S. Frittelli, T. P. Kling, and E. T. Newman, "Spacetime perspective of schwarzschild lensing," *Physical Review D*, vol. 61, no. 6, p. 064021, Feb. 2000, doi: 10.1103/PhysRevD.61.064021.